

4D Printing at the Microscale

Christoph A. Spiegel, Marc Hippler, Alexander Münchinger, Martin Bastmeyer, Christopher Barner-Kowollik, Martin Wegener, and Eva Blasco*

3D printing of adaptive and dynamic structures, also known as 4D printing, is one of the key challenges in contemporary materials science. The additional dimension refers to the ability of 3D printed structures to change their properties—for example, shape—over time in a controlled fashion as the result of external stimulation. Within the last years, significant efforts have been undertaken in the development of new responsive materials for printing at the macroscale. However, 4D printing at the microscale is still in its early stages. Thus, this progress report will focus on emerging materials for 4D printing at the microscale as well as their challenges and potential applications. Hydrogels and liquid crystalline and composite materials have been identified as the main classes of materials representing the state of the art of the growing field. For each type of material, the challenges and critical barriers in the material design and their performance in 4D microprinting are discussed. Importantly, further necessary strategies are proposed to overcome the limitations of the current approaches and move toward their application in fields such as biomedicine, microrobotics, or optics.

(refer to the selection of recent reviews in 3D printing technologies for further insight).^[5,11] Recently, 3D laser lithography, also known as direct laser writing (DLW), has become a powerful tool for the printing of precise and complex 3D architectures at the micro and nanometer scale.^[6–8] DLW relies on a multiphoton polymerization process using a femtosecond pulsed laser, which is tightly focused into a photoresist, allowing the fabrication of 3D structures with sub-micrometer resolution.

Although considerable progress has been made in the field, most of the materials and techniques currently employed for 3D printing are limited to the fabrication of static objects. Incorporation of “life” into the created 3D objects, often called 4D printing, is one of the current challenges.^[9–12] The additional dimension (time) refers to the ability of a 3D printed object to change its properties, such as shape or functionality,


over time in a controlled fashion, opening new possibilities that are not accessible with other technologies. One of the explored strategies relies on the use of adaptive materials, which are able to change their properties in a controlled manner upon an external stimulus.^[13,14] The most widely investigated stimuli are temperature, light, pH, or magnetic and electric fields. In the last few years, pioneering studies on the printing of time-evolving (4D) structures based on smart polymers at the macroscale have been reported.^[15,16] However, while the 4D printing of macroscopic objects^[9–12] (typically of a few centimeters in overall size) has

1. Introduction

3D printing has recently attracted significant attention not only in the basic sciences but also in industry.^[1–3] Today, different materials including ceramic, metals, polymers, and composites can be processed by 3D printing.^[4] Multijet modeling (MJM), fused deposition modeling (FDM), inkjet and aerosol jet printing, selective laser sintering (SLS), stereolithography (SLA), digital light processing (DLP), continuous liquid interface production (CLIP) are common examples of current 3D printing technologies

C. A. Spiegel, Prof. C. Barner-Kowollik, Dr. E. Blasco
Macromolecular Architectures
Institute for Technical Chemistry and Polymer Chemistry
Karlsruhe Institute of Technology (KIT)
Engesserstr. 18, 76128 Karlsruhe, Germany
E-mail: eva.blasco@kit.edu

C. A. Spiegel, Prof. M. Wegener, Dr. E. Blasco
Institute of Nanotechnology
Karlsruhe Institute of Technology (KIT)
Hermann-von-Helmholtz-Platz 1, 76344 Eggenstein-Leopoldshafen,
Germany

 The ORCID identification number(s) for the author(s) of this article can be found under <https://doi.org/10.1002/adfm.201907615>.

© 2019 The Authors. Published by WILEY-VCH Verlag GmbH & Co. KGaA, Weinheim. This is an open access article under the terms of the Creative Commons Attribution-NonCommercial License, which permits use, distribution and reproduction in any medium, provided the original work is properly cited and is not used for commercial purposes.

M. Hippler, A. Münchinger, Prof. M. Wegener
Institute of Applied Physics
Karlsruhe Institute of Technology (KIT)
Wolfgang-Gaede-Str. 1, 76131 Karlsruhe, Germany

M. Hippler, Prof. M. Bastmeyer
Zoological Institute
Karlsruhe Institute of Technology (KIT)
Fritz-Haber-Weg 4, 76131 Karlsruhe, Germany

Prof. M. Bastmeyer
Institute of Functional Interfaces
Karlsruhe Institute of Technology (KIT)
Hermann-von-Helmholtz-Platz 1, 76344 Eggenstein-Leopoldshafen,
Germany

Prof. C. Barner-Kowollik
School of Chemistry
Physics and Mechanical Engineering
Queensland University of Technology (QUT)
2 George Street, Brisbane, QLD 4000, Australia

DOI: 10.1002/adfm.201907615

been achieved, 4D printing at the microscale is still in its infancy. Hence, in the current progress report we summarize the state of the art with regard to this emerging field of 4D microprinting with special focus on the material design. In addition, the critical challenges that need to be overcome to enable their application in fields such as biomedicine, microrobotics or optics, where a controlled response and adaptivity to external stimuli is essential, are analyzed and discussed (Figure 1).

2. Hydrogels in 4D Microprinting

Hydrogels are hydrophilic polymer networks that can absorb large amounts of water. They are widely used in the biomedical field because of their low cytotoxicity and favorable properties to mimic the extracellular matrix of connective tissues.^[17,18] Due to their high water content, cells or tissue can be supported with solvated nutrients from all directions compared to conventional cell culture dishes. Importantly, the stiffness can be well adjusted to regimes that are aligned with the physiological conditions-dependent on the cell type. Furthermore, in some special cases cells can infiltrate the hydrogel matrix, grow there and even reorganize it. However, to mimic the natural cellular environment in living organisms, dynamic systems which can be adapted to changes in the cells are required. While the use of stimuli-responsive hydrogels is already well-established in the biomedical field, most of the applications are on the macroscale.^[13,19–22] Thus, 4D hydrogel-based microstructures are an emerging field with the promise to tailor geometrically defined, yet dynamic environments for the study of single cells and tissue.^[23]

A second interesting research field for stimuli-responsive hydrogels is soft robotics. Here, the major aim is to fabricate robotic elements with soft and elastic materials to approach the situation in living organisms. Stimuli-responsive hydrogels are an excellent choice for the application in aqueous environments and thus widely used (see also Section 4.2.).^[24] The ability to move to 4D microstructures has opened new possibilities in this area, already leading to promising applications like microgrippers^[25,26] or microactuators^[27–29] (see further examples in Section 2.2.).

2.1. Challenges in the Material Design and Microprinting

For the fabrication of stimuli-responsive hydrogel micro- and nanostructures, 3D laser lithography is the preferred technique. Thus, the development of suitable photoresists is imperative. Typically, they are composed of three main constituents: stimuli-responsive monomers, crosslinkers and a photoinitiator—all solved in an appropriate solvent (Figure 2).

Incorporation of the stimulus-response is usually accomplished by selecting the adequate monomer. Stimuli-responsive monomers containing acrylamides or acrylates and functional groups (e.g., carboxylic acid, amines, etc.) are common examples (see Section 2.2. for further details in concrete examples). These monomers can be photopolymerized with the laser due the presence of acrylates or acrylamides on one hand, and on the other hand, they exhibit a response to an external stimulus (e.g., pH or temperature) due to the presence of the functional group. In order to achieve mechanically stable hydrogel structures, the



Christoph A. Spiegel received his M.Sc. degree in chemistry from Swiss Federal Institute of Technology in Zurich (ETH Zürich), Switzerland in 2018. He is currently a Ph.D. candidate in the Institute of Nanotechnology (INT) at the Karlsruhe Institute of Technology (KIT) in the group of Dr. Eva Blasco. His research interests mainly focus on the design and preparation of new photoresists for 4D microprinting.



Eva Blasco completed her Ph.D. studies in 2013 at the University of Zaragoza (Spain) under the supervision of Prof. L. Oriol and Dr. Pinol. Thereafter, she obtained an Alexander von Humboldt Postdoctoral Research Fellowship to work in the groups of Prof. C. Barner-Kowollik (Polymer Chemistry) and Prof. M. Wegener (Applied Physics) at the Karlsruhe Institute of Technology (KIT) in Germany on the preparation of 3D conductive microstructures via 3D laser lithography. Since 2016, she has been working as a scientist at KIT. Her research interests include the development of new functional materials by employing light, particularly, for 3D laser lithography.

addition of a crosslinker, i.e., monomer containing two or more photopolymerizable groups, is necessary. In contrast to conventional photoresists, the amount of additional crosslinker is critical to maintain their stability and functionality. Since most of the systems rely on a swelling (or shrinkage) of the hydrogel upon stimulation, actuation is strongly suppressed if the network is too stiff. Thus, the ratio functional monomer/crosslinker needs to be carefully optimized.

The photoinitiator is an important component of the system to be considered, too. A well chosen photoinitiator for the fabrication of hydrogel-based microstructures features a high two-photon cross-section and has to be soluble in the water or polar solvent, common media in hydrogels. The latter requirement is more challenging to fulfill, although some efforts have been already published concerning the development of water soluble two-photon initiators.^[30,31] In addition, low cytotoxicity of the photoinitiator is also crucial, especially for biological applications.

In terms of fabrication, the gray-tone lithography approach has been exploited for the preparation of complex responsive hydrogel-based microstructures.^[25,29,32,33] Gray-tone lithography allows for tuning the resulting properties of a material

4D Microprinting

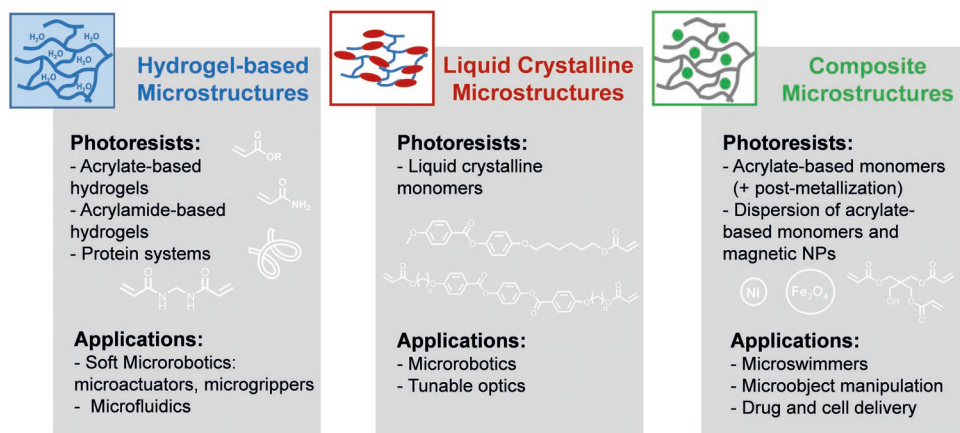


Figure 1. Overview of the emerging materials for 4D printing at the microscale and their current applications.

during the fabrication by altering the exposure dose, e.g., by adjusting the laser intensity. Briefly, by increasing (or decreasing) the exposure dose during the writing process, the crosslinking density of the polymer network increases (or decreases), which results in changes of the properties of the fabricated structures, e.g., thermal expansion coefficient or Young's modulus.^[34,35] In the case of hydrogels, the effect is significantly stronger due to the high impact of the crosslinking density on the stimuli-response of the final structure, as described above. Thus, gray-tone lithography can be employed to create different effective hydrogel-based materials from the same photoresist during a single fabrication

step. In contrast to hydrogel microstructures fabricated with constant writing parameters, where only isotropic swelling or shrinkage is possible, gray-tone lithography enables heterogeneous structures able to execute more complex movements (see examples below).

2.2. Stimuli-Responsive Hydrogel-Based Microstructures

As noted above, the most common stimuli studied in 4D microprinting of hydrogels are temperature, pH or solvent. Hydrophilic polymeric networks based on acrylamides or acrylates and proteins in some few examples have been mainly employed in the fabrication. In this section, we provide a short review of various examples of the stimuli responsive microstructures based on hydrogels.

2.2.1. Acrylamide-Based Hydrogels Microstructures

A prominent group of responsive materials are hydrogels based on poly(*N*-isopropylacrylamide). They exhibit drastic volume changes by taking up or releasing significant amounts of water from the polymer network. On the other hand, other stimuli-responsive monomers such as acrylic acid are often combined with acrylamides, which serve as backbone with good water solubility. Additionally, *N,N'*-methylene bisacrylamide is commonly employed as a crosslinker to achieve sufficient structural stability.

In a pioneering study in 2002, Watanabe et al. demonstrated a photoresponsive hydrogel microstructure fabricated by 3D laser lithography.^[36] They used a comonomer solution of acryloylacetone, acrylamide

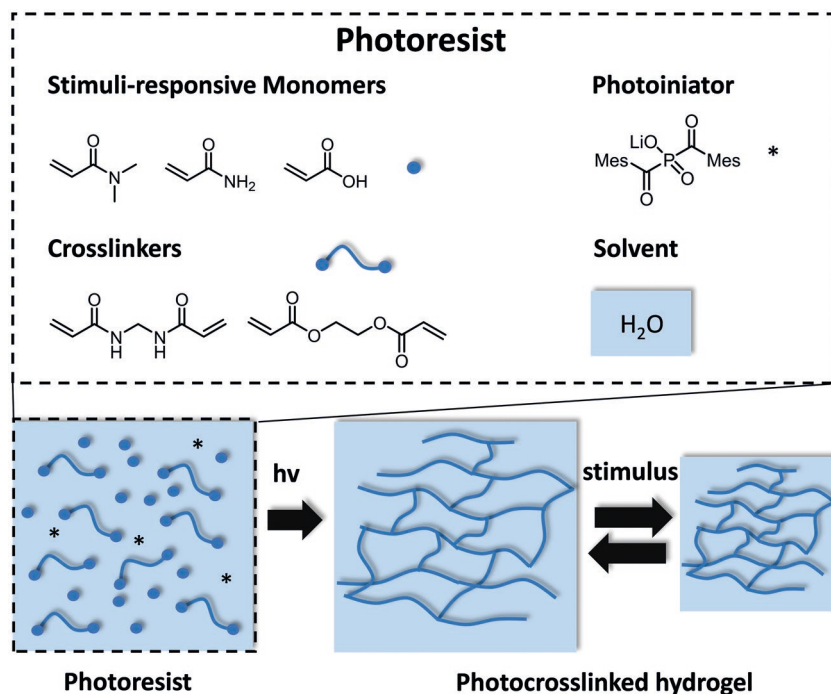


Figure 2. Schematic representation of the components of hydrogel-based photoresists as well as their photocrosslinking and actuation processes.

and *N,N'*-methylene bisacrylamide as a crosslinker. The photoresponse was achieved by illumination with 244 nm wavelength UV light, leading to a photoexcitation of the acetylacetonate groups and subsequent swelling of the hydrogel. Based on this system, they first investigated the impact of the acryloylacetonate content on the stimuli-response in polymer films and found a significant increase of swelling by increasing the number of functional groups. Furthermore, they studied the material response (swelling) over time, with a saturation after about 2 h of illumination—independent on the acryloylacetonate content. However, they concluded that the process is ultimately governed by diffusion and thus highly dependent on the structure size which was relatively large in their experiments. Thus, a faster response is expected for smaller structures. With the optimized resist composition, these authors utilize two-photon lithography to fabricate 3D microstructures. In their writing strategy, they use the “gray-tone” approach to alter the strength of the stimuli-response in a single photoresist. This enabled them to fabricate a bi-layered microcantilever with a less-crosslinked and thus more sensitive side on the bottom. Upon illumination with UV light, the lower side experienced a significant swelling, which leads to an upward bending of the cantilever by about 45°. Although the process was essentially irreversible and the structure was fairly large, they presented the first example of photoresponsive 3D microstructures. Importantly, the study discusses several of the key aspects, such as the importance of the resist composition and its strong impact on the response, which are now commonly applied in the micro-fabrication of stimuli-responsive hydrogels in general.

Xiong et al. demonstrated a solvent-driven micropump^[37] using 2-acrylamido-2-methylpropane sulfonic acid sodium salt, acrylamide and *N,N'*-methylene bisacrylamide as a crosslinker.

The resulting material is sensitive to swelling with different solvents. These authors exploited the swelling effect by putting a hydrogel film between two reservoirs of solvents, which leads to a bending of the hydrogel if different solvents are on both sides of the film. In this manner, they created a micro-pump with two different materials. Initially, they fabricated a solid microchannel with a commercially available acrylate resist and second, they added a valve and a thin film with the stimuli-responsive hydrogel. By exchanging the solvent from water to ethanol they observe a deflection of the thin hydrogel film within hundreds of milliseconds. They also showed a completely reversible behavior when they change the solvent back to water, enabling the pumping of very low volumes. Even though the exchange of solvents as a trigger is a relatively slow process, they describe a possible extension of their approach to micropumps driven by other stimuli such as pH level or temperature.

In a follow-up work, the same group utilized the gray-tone approach to achieve asymmetric hydrogel microstructures^[25] and studied the swelling behavior as a function of NaCl concentration (Figure 3A). The main emphasis, however, was on the investigation of the gray-tone technique to control the crosslinking density with a high spatial resolution. These authors explored the bending angle as a function of the writing parameters in bimaterial structures and find a tuning window to achieve different responses. Further, they made use of the freedom in design of the 3D laser lithography technique and put two bimaterial beams with opposite writing parameters next to each other to form a simple gripper.

Zarzar et al. reported the fabrication of pH- and temperature responsive hydrogel patterns onto polymeric micropillars^[27] employing *N*-isopropylacrylamide (temperature responsive) and acrylic acid (pH responsive) as stimuli-responsive monomers

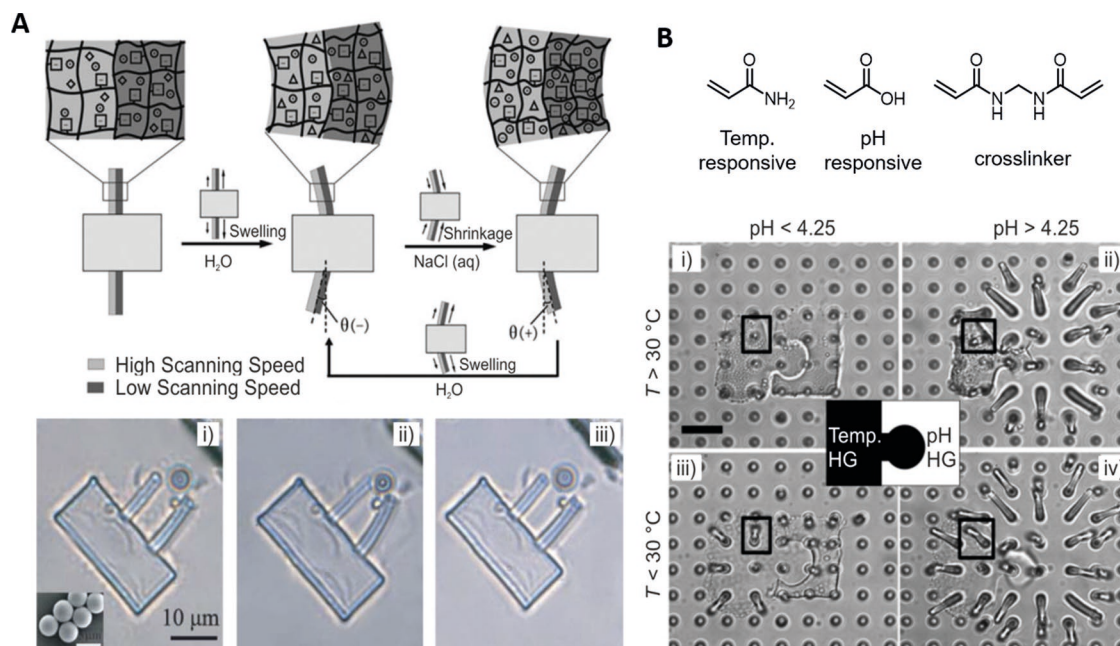


Figure 3. A) Schematic illustration of the gray-tone approach to prepare responsive hydrogel-based microstructures (top). The variation in scanning speed leads to different responses to solvent changes, thus enabling a microgripper to trap and release particles (i–iii). B) Temperature- and pH-responsive hydrogels fabricated as interlocking puzzle-pieces (center). Optical micrographs show different response to combinations of temperature and pH. Adapted with permission.^[25,27] Copyright 2011, ACS and Wiley-VCH.

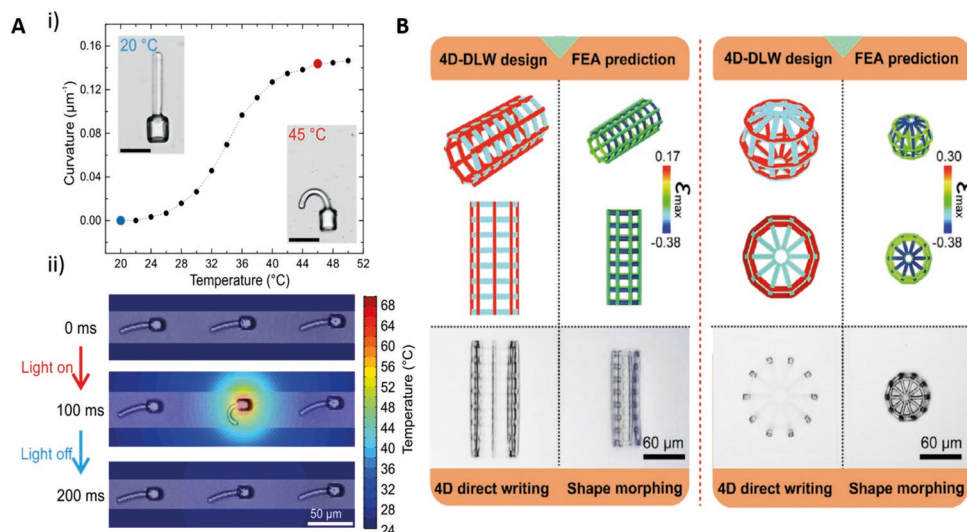


Figure 4. A) Characterization of poly(*N*-isopropylacrylamide) based hetero-microstructures as a function of temperature and light. i) Curvature, i.e., inverse radius versus temperature. ii) Fast light-induced actuation by exploiting two-photon absorption induced heating using a focused femtosecond laser on one of the structures. A calculated temperature profile with false-color scale is overlaid onto the optical micrographs. B) Complex actuation based on 4D direct laser writing. Finite element analysis (FEA) is applied to predict the desired transformation and model the structures accordingly. A stent and a cage structure with large and reversible deformations are demonstrated with the according FEA calculations. Adapted with permission.^[29,32] Copyright 2019, Springer Nature and Elsevier.

(Figure 3B). Hydrogel pads were fabricated onto polymeric pillar arrays and a strong displacement of the pillars upon swelling of the hydrogels was observed. This concept highlights the ability to use the hydrogel as an active element to exert force and bend other, nonresponsive elements. Furthermore, the authors combined both hydrogels into a composite structure and showed the independent response to the respective stimulus. The hydrogels based on *N*-isopropylacrylamide displayed a large swelling response upon small changes in temperature around 30 $^{\circ}\text{C}$. This mild stimulation compared to changes in pH is especially interesting in the context of cell culture applications.

Recently, some of us presented a new strategy for the fabrication and actuation of microstructures based on poly(*N*-isopropylacrylamide).^[29] First, the fabricated microstructures fabricated via 3D laser lithography were characterized via atomic force microscopy (AFM) to assess the swelling and the change in Young's Modulus as a function of temperature (Figure 4A). In a first application example, we combined this stimuli-responsive hydrogel with conventional rigid materials to create a valve for microfluidic microchannels. With these valves, the open area of the channel can be reversibly adjusted as a function of temperature. As a second step, we utilized the gray-tone approach to create 3D bimaterial beams from a single photoresist and characterized different design parameters on the response. As an important step toward future applications, we proved that this fabrication technique is robust and that the response is completely reversibly without deterioration. Furthermore, we demonstrated that arbitrary and complex actuations can be obtained when the structure with more and less crosslinked parts is appropriately designed. These results were supported by numerical simulations, which reliably reproduced our experimental data with given material parameters. For many practical applications, it is desirable to not only stimulate the entire

structure by a global change in temperature, but to exclusively trigger specific parts of a structure. To achieve this goal, we exploited a local two-photon absorption induced photothermal heating by a focused pulsed laser beam (Figure 4A). With this system, we were able to address individual structures and demonstrated a strong and fast response in the order of 100 ms.

In the same year, Chen and co-workers published their work on 4D reconfigurable compound machines^[32] employing the well-known monomers, *N*-isopropylacrylamide and acrylic acid (Figure 4B). The resulting material exhibited significant responses to changes in temperature and pH value. In their fabrication processes, the gray-tone approach was employed and an extensive analysis on the writing parameters and the influence on the swelling behavior was conducted. As a result, the strong dependence between the crosslinking density (measured as the material stiffness) and the stimuli-response was clearly shown. One key aspect of their work was the ability to create sophisticated 4D designs based on numerical calculations. The authors used this tool to predict the response and adjust the fabrication design to achieve the desired outcome. Utilizing this system, elaborated examples like stents or cage structures that dynamically change their size were successfully fabricated. Since the strongest responses were only achieved with significant changes in pH, potential applications are limited due to the harsh stimulus. Their proposed workflow to model the response and adapt the fabrication design, however, is powerful and might be readily transferred to other materials and stimuli.

2.2.2. Acrylate Based-Hydrogels Microstructures

Acrylate based photoresists are widely used in the field of 3D laser lithography due to their efficient polymerization in a

presence of a photoinitiator. In the field of hydrogels, water soluble acrylic monomers have also been successfully incorporated in photoresists. Monomers such as poly(ethylene glycol) diacrylate (PEGDA) or ionic-liquid monomers containing acrylate groups have been exploited for the preparation of responsive microstructures based on hydrogels.

Tudor et al. presented stimuli-responsive microstructures based on poly(ionic liquid)s.^[38] They were able to fabricate structures with high writing speeds and sub-micrometer resolution which respond to changes in temperature. The response was monitored using a microheater. Significant volume changes were found between 20 and 70 °C. One interesting aspect was the possibility to dry the samples, since hydrogel structures are typically destroyed when the water is removed from the polymer network.

Also, Lv et al. reported humidity responsive hydrogel microstructures via 3D laser lithography.^[39] A photoresist consisting of PEGDA with a photoinitiator to generate a hydrophilic polymer networks which can absorb and desorb large amounts of water reversibly was employed. The authors characterized the swelling as a function of writing parameters and exploited the correlation between exposure dose and structure response to optimize der structures. Based on this system, several demonstrations that could serve as humidity sensors or form actuators in soft robotics were shown.

2.2.3. Protein-Containing Systems

Another promising and special class of stimuli responsive microstructures is based on proteins. They are especially attractive for biomedical applications because of their inherent biocompatibility and biodegradability.^[40]

Kaehr and Shear reported the preparation of responsive protein hydrogel-based microstructures employing available proteins BSA, avidin, and lysozyme with different swelling properties as a function of pH values.^[33] In one of their initial studies, these authors demonstrated the ability of two-photon lithography to reach 3D features with sub-micrometer resolution for stimuli-responsive hydrogels. By combining different proteins, the swelling response of the resulting microstructures was tuned over a wide range. Importantly, they showed that this process is completely reversible by cycling between different pH values. By applying the gray-tone approach, a local modification of the crosslinking density at the microscale was achieved and consequently, bimaterial structures which bend in response to changes in pH were demonstrated. In a proof of concept experiment, *Escherichia coli* bacteria were trapped in a microstructure and subsequently released upon stimulation of the protein hydrogel. While proteins as a base material offer good biocompatibility, the applied pH changes were still harsh. To open a larger field of applications, especially for mammalian cells, they suggested modifications to induce the volume changes by ligands in solution.

Recently, Lee et al. reported shape shifting 3D BSA protein microstructures which respond to changes in pH.^[26] The authors of this work demonstrated microstructures with sub-micrometer resolution and investigated the swelling response as a function of geometry and fabrication parameters. By

adjusting the layer distance during the writing process, an effective change the exposure dose was achieved, thus exploiting the gray-tone approach to modify the response of their structures. AFM was employed to characterize the mechanical properties and correlate them with the swelling properties they observed in optical micrographs. On this basis, bimaterial beams with a bending response and ultimately a gripper with four arms, able to open and close as a response to changes in pH, were successfully shown.

2.3. Outlook

Stimuli-responsive hydrogel microstructures are a research field with promising future applications. The fact that they rely on an aqueous environment might limit their possibilities of operation, but makes them particularly valuable in the biomedical area. One important aspect that has been exploited extensively is the ability to control the strength of the material response via gray-tone lithography. With this technique, it is possible to create a multitude of different effective materials in a one-step procedure from a single photoresist. However, it has to be noted that the crosslinking density is directly connected to the structure stability and therefore, a careful design is required to obtain optimum results.

As a next step, it will be important to focus on the main challenges to bring the research field forward. The majority of the work so far has been focused on sophisticated demonstrations, but the critical next move will be the application of these promising materials and techniques in real examples, e.g., single-cell manipulation or soft robotics.

Since the main potential applications lie in the biomedical area, further efforts on the development of new materials ensuring biocompatibility, along with a controlled response, are essential. While many stimuli-responsive hydrogels are generally nontoxic in the polymerized state, photoinitiators and monomers employed for the fabrication might affect or harm the biological systems. Thus, the impact of residual unreactive monomers or photoinitiators remaining in the microstructures needs to be further investigated. In addition, materials and consequently, the fabricated microstructures able to respond to mild stimuli are highly desired. Interesting candidates for this task are visible light and chemical or enzymatic triggers which do not influence cellular behavior. For example, photoreversible immobilization of proteins, enzymes and growth factors to hydrogels with excellent spatiotemporal resolution while retaining native protein bioactivity might become a reality. Moreover, hydrogel microstructures able to respond to several external stimuli in a spatial and temporal controlled manner will open new possibilities in biological studies that are currently unattainable.

3. Liquid Crystalline Materials in 4D Microprinting

Liquid crystals (LCs) are a state of matter in between the crystalline and the fluid phase. There are various types of liquid-crystal phases (called mesophases), which can be characterized by the type of long-range order, either positional or orientational

order. One of the most common phases is the nematic phase. It is usually characterized by stiff rod-shaped molecules, which are randomly distributed in space but aligned along a common direction, which is called the director.^[41]

An interesting class of LCs are liquid crystal elastomers (LCE) consisting of a crosslinked liquid crystalline polymer network which combines the entropy elasticity of an elastomer with the self-organization of the liquid crystalline phase showing a long-range order as described above.^[42] LCE are attractive candidates in 4D printing due to their ability to undergo a change in the order parameter (reorientation of the molecules), which can lead to a large mechanical actuation. A single crystal LCE contracts along the director and expands along the orthogonal directions.^[42] Such a single crystal can lift thousand times its own weight on actuation. By imprinting more difficult director distributions, more complex movements, for example bending, can be achieved.^[43]

LCE has been extensively explored for the fabrication of actuators at the macroscale.^[44] However, in recent years, interest has grown in these materials for 3D printing at the microscale. Below, we will focus on the challenges as well as on the potential of these materials for applications such as microrobotics or tunable optics.

3.1. Challenges in the Material Design and Microprinting

To tailor 4D microstructures with arbitrary shape and motion, one has to face three major challenges. First, a versatile technique is required to realize any shape of the polymer in space. Second, it is crucial to control and fix the director field during the fabrication process inside the polymer to program the desired motion. Third, a suitable trigger to manipulate the order parameter, and therefore the motion, has to be included. All three challenges can be faced in a 3D printing process starting from a resist containing functionalized mesogenic units that can be photopolymerized.

Presently, two main methods are employed for the fabrication of liquid-crystalline microstructures: i) direct ink writing (DIW)^[45] and 3D laser lithography.^[46,47]

In DIW, a viscous LCE resist is pushed through a fine nozzle which moves above a substrate and is thereby capable to print 3D structures with feature sizes of a few hundred micrometers. The shear forces that act on the resist during the printing process align the director along the print path.^[45] In a final step, the resist is polymerized by a UV lamp and thus the alignment of the director is fixed. The difficulty in DIW is to design a proper ink that has the right viscosity in the nematic phase. This is achieved by Michael addition of LC diacrylates with *n*-butylamine^[43,45,48] or EDDT.^[49] The latter makes it possible to print the resist at room temperature, while resists based on *n*-butylamine have to be printed at elevated temperatures to obtain the required viscosity. With DIW of LCEs, a few nice but macroscopic examples have been realized, for example a gripper, an artificial hand, folding structures^[43,45,49] and simple adaptive optics.^[48] In all of these examples, the used trigger is simply induced disorder by heating.

In contrast to DIW, submicron feature sizes are possible using the already mentioned two-photon lithography technique.

Typically, the employed photoresists for this technique are composed of a LC monomer, a crosslinker (usually a diacrylate containing the mesogen), and a photoinitiator.

As mentioned above, the alignment of the LC molecules is important to achieve the desired actuation. Alignment is usually achieved via treatments of the glass substrates that sandwich the resist to enforce the alignment at the surface. The director field inside of this cell is then given by the minimization of the Frank-Oseen free energy.^[50] This process is referred to as surface-mediated alignment in contrast to bulk-mediated alignment, where body forces are applied to directly manipulate the director inside of the cell. To achieve alignment parallel to the substrate, thin polyimide (PI) or polyvinyl alcohol (PVA) layers are rubbed with a cotton cloth to create microgrooves on the surface.^[47] Vertical alignment is usually attained via special PI coatings^[51–53] or treatments of the glass surface with silanes.^[54] Thereby, it is possible to obtain a homogeneous vertical^[51,53] horizontal^[55] or a splayed director field^[52] in the bulk of the cell.

A more sophisticated method for director alignment has been reported by Tartan et al. They combined surface mediated alignment with an electric field (bulk mediated alignment) inside of a sandwich cell formed of two coated glass substrates. Spatial and temporal control of the director field is obtained during the writing process throughout the whole cell.^[56] In detail, they added a transparent and conductive layer between the glass substrate and the alignment layer. Therefore, an electric field in the vertical direction can be applied. The molecules of a nematic solvent with high dielectric anisotropy align along this field and in turn align the used mesogenic monomers. With that technique, it was possible to switch from homogeneous horizontal alignment mediated by the surface to a splayed alignment, while the distance needed for the turn of the director decreases with higher electric fields. Exploiting the temporary twisted state during the relaxation to the horizontal alignment after voltage shutdown, also horizontally twisted director fields can be achieved in the polymerized LCE.

3.2. Liquid-Crystalline Microstructures

In the following, we will present recent examples focused on LCE microstructures using two-photon lithography. The photoresist employed in the succeeding examples consists of a mesogenic monomer equipped with an acrylate group (1), the mesogenic crosslinker (2), and Irgacure 369 (4) as photoinitiator, as shown in (Figure 5). The ratio of (1) to (2) heavily influences the mechanical properties of the LCE as for example the Young's modulus or the possible actuation of the material.^[57,58] To trigger the actuation by light, 1 wt% of the azobenzene dye (3) was also typically included in the resist. It is synthesized to minimize one-photon absorption and two-photon absorption of the writing laser during the 3D printing process. Furthermore, it is equipped with an acrylate group to be covalently incorporated into the LCE. Upon irradiation with green light, the azobenzene dye can be switched from *trans* to *cis* configuration, from where it quickly relaxes back by a thermal process.^[59] This process caused actuations of up to 20% strain in homogeneously aligned actuators^[55,57] on the timescale of several milliseconds.^[59,60]

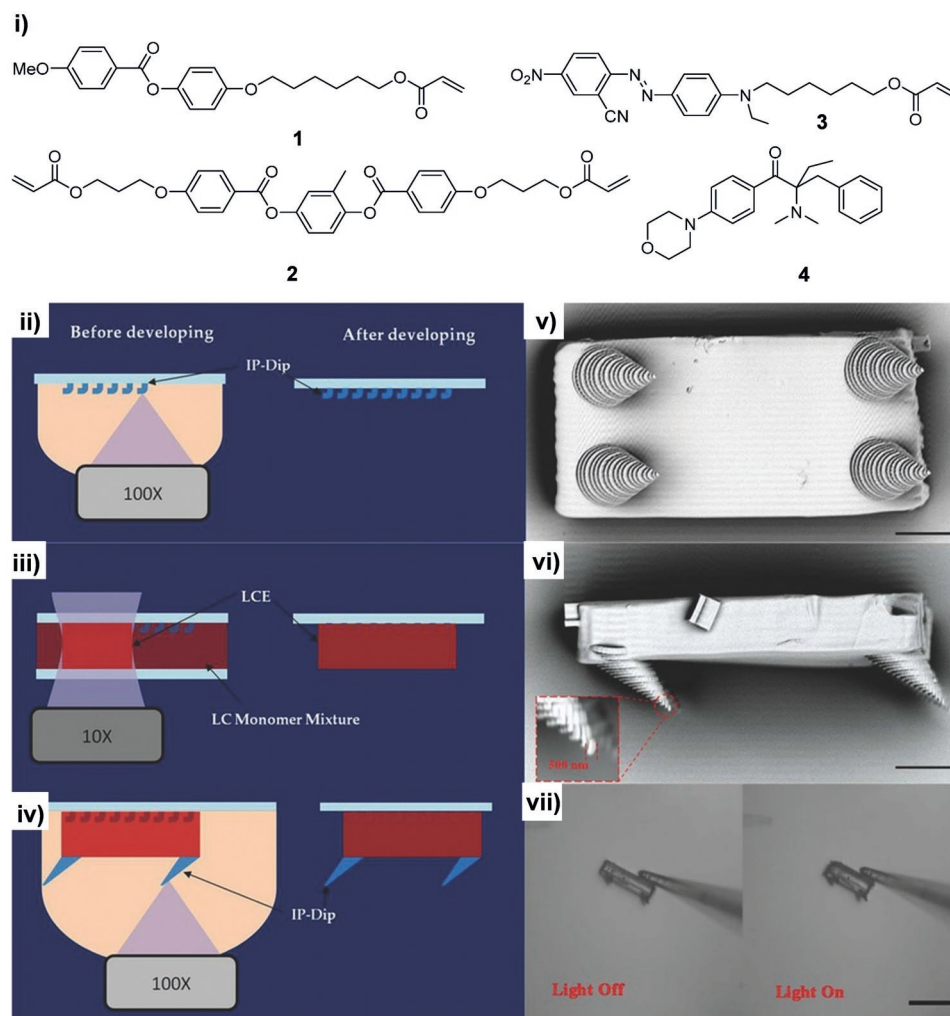


Figure 5. i) The constituents of the LCE resist employed in the highlighted examples are depicted. Monomer (1) is a mesogenic unit with one acrylate group, which forms polymer strings on polymerization, while the mesogenic monomer (2) crosslinks them to form a stable network (LCE). The azo-dye (3) is also incorporated into the network and is used to induce heating via light and thus triggering deformations. The photoinitiator (4) starts radical polymerization during the printing process; ii) Microscopic walker. Anchors were printed on a PVA coated substrate with a commercially available resist (IP-Dip, Nanoscribe GmbH) to support the LCE body of the walker during the fabrication; iii) The LCE body was printed in a second step on top of the anchors; iv) In a third step the legs of the walker were printed with IP-Dip; Scanning electron beam photograph of the walker in bottom view (v) and in side view (vi) (scale bar = 10 μm); vii) Optical microscope image of the walker attached to a fiber in the relaxed state on the left hand side and the contracted state on the right (scale bar = 50 μm). Adapted with permission.^[55] Copyright 2015, Wiley-VCH.

3.2.1. Robotics

Zeng et al. presented a microscopic walker that is able to overcome the van der Waals force between its legs and the surface it walks on.^[55] As depicted in Figure 5ii–vii, the walker consists of a homogeneously aligned LCE body ($60 \times 30 \times 10 \mu\text{m}^3$) with slightly tilted legs attached to it, while the legs are printed with a rigid, commercially available acrylate resist called IP-Dip (Nanoscribe GmbH). Shining green light onto the walker, the body contracts and thus the legs move toward each other in the line of the director, as shown in Figure 5vii. Removing the laser light, the body relaxes again and the legs move apart. Since the legs are tilted, one direction of movement is easier for the legs and therefore the walker moves forward during one cycle of illumination. The fabrication was accomplished by

using a multistep process as illustrated Figure 5ii–iv. In a first step, one glass of the cell was spin coated with a PVA layer and rubbed afterward to ensure horizontal alignment of the LCE resist. In a second step, anchors were printed via 3D laser lithography onto this glass with IP-Dip to ensure proper fixation of the LCE body to the substrate during fabrication. Subsequently, the cell was closed with a second glass that was coated with a rubbed PI layer and capillary filled with the LCE resist described above. Afterward, the body of the walker was written, again via 3D laser lithography. In a last step, the cell was opened and the legs were written using IP-Dip as a photoresist. Finally, the whole walker was detached from the glass substrate.

A more sophisticated robot was reported by the same group.^[52] There, the LC photoresist was employed to build an optically controlled microhand. The fingers of the hand

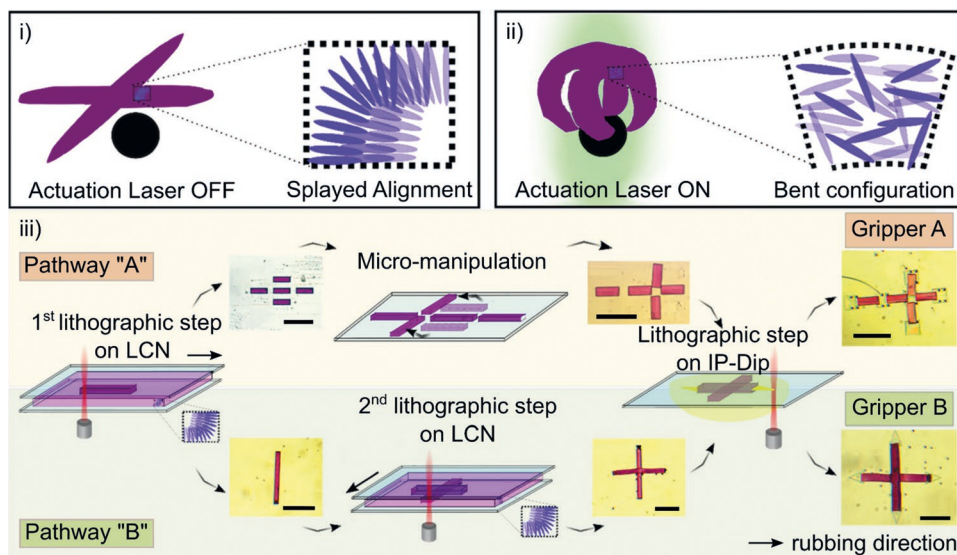


Figure 6. i) Schematic representation of the microgripper in the relaxed state. The splayed orientation of the molecules is sketched in the inset to the right; ii) Schematic representation of the contraction of the microgripper under irradiation with a laser. The inset shows the new reorientation of the molecules inside of the material; iii) Two possible fabrication pathways of the microgripper (scale bar = 100 μm). Adapted with permission.^[52] Copyright 2017, Wiley-VCH.

consist of a LCE with a splayed director field, thus they bend on irradiation with green light, similar to a bimetal beam on heating as depicted in **Figure 6i,ii**. A microgripper which can be freely positioned in space and actuated by light via a fiber was achieved. For the fabrication, the authors reported two distinct methods as displayed in **Figure 6iii**. In both methods, a cell was prepared from a rubbed PVA coated glass and a PI coated glass to achieve a splayed director field inside. Since the director at the PVA coated glass must point along the finger during the writing to achieve a bending, the hand cannot be written in one step. Either, the microfingers (around 60 μm long) have to be printed all along the director in the cell and afterward be rearranged (Pathway "A") or the PVA coated glass has to be rotated during the fabrication (Pathway "B"). In a last step, the "finger nails" of the hand were printed with IP-Dip that reduce the van der Waals force at the end of the fingers and therefore ensure that the hand opens again after gripping.

3.2.2. Tunable Optics

The controllable shape change of the LCE-based microstructures is also useful for tunable optical devices. A prominent example is whispering gallery mode resonators (WGM) whose resonance frequency can be shifted by an optical stimulus. Flatae et al. reported a goblet type PMMA resonator, which is filled by a cylinder of LCE (25 μm diameter, 10 μm height) that stretches the resonator on irradiation to shift the resonance frequency.^[51] The director of the LCE is thereby along the symmetry axis of the resonator to achieve a symmetric distortion. The LCE cylinder was printed in a LCE cell as described above with a PI coating to obtain an alignment perpendicular to the glasses of the cell. Afterward, the cylinder was removed from the cell and positioned with a micromanipulator inside of a PMMA resonator (45 μm diameter). Using heat treatment, the

actuator was welded to the resonator. A more direct approach to obtain a tunable WGM is to print it directly from LCE via 3D laser lithography as described by Nocentini et al.^[53] A micrometric resonator based on LCE close to a waveguide (2 μm thick and 2.5 μm wide) was also fabricated via 3D laser lithography using IP-Dip for easy coupling to the resonator.

Another application worth mentioning are a tunable gratings, for which the diffracted orders can be positioned in space by adjusting the grating constant via laser heating as described above.^[60,61] Such gratings can also be exploited to manipulate the polarization state of the diffracted light.^[61,62]

3.3. Outlook

The use of LCE based photoresists is one of the most promising approaches for obtaining dynamic microstructures operating under ambient conditions with potential applications in the fields of microrobotics and optics. Nevertheless, further improvements are still necessary. The presented microstructures were limited to the height of the used sandwich cell. However, many interesting microstructures have been presented in the past that are far beyond this limit, for example in the field of mechanical metamaterials.^[63] In addition, all examples presented in this section employed the same liquid crystal photoresist formulation based on nematic LCs. Thus, there might be a huge potential if one would be able to incorporate new LCEs into this kind of structures to create responsive microstructures. Furthermore, achieving more complicated director profiles is currently difficult since multistep processes are required. To overcome all these limits, we believe that a flexible technique relying only on bulk mediated alignment is required in order to obtain complete control of the director during printing in cells with variable heights. This will open a new range of possibilities in the fabrication of complex LCE microstructures.

4. Composite Materials in 4D Microprinting

Preparation of composite and multimaterial structures by combination of two or more materials provides access to devices exhibiting new promising properties. Main contributions in 4D printing at the microscale using composites and multimaterial structures have been located in the field of magnetically actuated microrobotics with a focus on microswimmers and microtransporters. One of the main advantages is that magnetic fields with small amplitude and low frequency are harmless for living organisms. Furthermore, magnetic fields can penetrate water and tissue, enabling remote control.

4.1. Challenges in the Material Design and Microprinting

3D laser lithography has been employed as one of the main methods for fabrication of multimaterial 4D microstructures in recent years. As mentioned above, magnetically actuated microrobots are the principal application using composite materials. To achieve actuation, three main aspects need to be optimized: i) material composition, ii) geometry of the microstructure, and iii) stimulus applied, especially the type of magnetic field in this case.

Typical photoresists employed for the fabrication of magnetically responsive structures consist of two main components: multifunctional monomer, which allows for 3D printing, and magnetic material, which enables the response. The magnetic material can be either added after printing^[64–66] or incorporated during writing.^[67–69] In the first approach, the target structure is printed by 3D laser lithography using a polymer-based photoresist and subsequently post-modified by thin-film coating or surface functionalization with nanoparticles to incorporate the response. Very often coatings of nickel are used.^[64,70–72] In the second approach, 4D micro-objects are directly printed using composite photoresists which are usually composed of a mixture of monomers and magnetic nanoparticles, such as iron oxide.

Scaling of physical effects has to be taken into account for the design of microrobots. Although the microscopic world is governed by the same physical laws as the macroscopic world, the relative importance of different processes may vary strongly. For example, a change of the object size toward the microscale has dramatic consequences on the applied locomotion strategy in fluids. Microrobots exhibiting sizes in the range of several micrometers operate under conditions of low Reynolds (Re) numbers. For microrobots, having characteristic lengths and velocities in the range of 10^{-6} to 10^{-4} m, the Re number reaches values far below 1 in water. Under these conditions, inertial forces become negligible and viscous drag forces of the liquid dominate. Consequently, reciprocal motion, as shown by Purcell in his Scallop theorem, results in negligible net motion. Effective locomotion is only possible by nonreciprocal motion strategies.^[73] Facing these conditions, microorganisms have adopted several strategies for nonreciprocal motion such as the flexible beating flagella of spermatozoa or the screw-like motion by rotating helical flagella of *E. coli* bacteria. Thus, design and locomotion of artificial microrobots have been strongly influenced by these optimized biological designs.

The type of applied field depends on the design of the microstructures and needs to be carefully optimized to achieve the

desired actuation. For example, for helical microswimmers temporally constant, rotating magnetic fields (RMF) are used, inducing a torque, which acts to align the swimmer's magnetization with the magnetic field. This generates rotation along the helical axis, which is translated into translational motion. Raising the RMF frequency increases forward velocity until the step-out frequency is reached. At this frequency the applied magnetic torque is not strong enough to keep the microrobot synchronized with the field, resulting in abrupt decrease of forward velocity.^[74] In case of cage-like geometries magnetic gradient fields are utilized, applying a magnetic force on the object, which induces locomotion.

4.2. 4D Composite Microstructures

As mentioned above, most of the systems based on composite materials consist of magnetically actuated microrobots. In the following, the most prominent examples with special focus on their application will be presented.

4.2.1. Helical Microswimmers

Inspired by the design of bacterial flagella, microstructures exhibiting a chiral helical architecture, very often called microswimmers, allowing locomotion by corkscrew motion have been extensively investigated. In 2012, Tottori et al. established the first protocol for preparation of helical microswimmers using 3D laser lithography.^[64] They developed a simple and general fabrication procedure including printing of the helical structure from negative photoresists such as SU-8 and IP-L (Nanoscribe) as first step. Subsequently, the helical microswimmers were coated with a Ni/Ti bilayer via electron beam evaporation. Different microstructures with lengths ranging from 4 to 64 μm with examples featuring microholders were fabricated. The swimmers achieved speeds of $320 \mu\text{m s}^{-1}$ and showed no cytotoxicity in biocompatibility tests. In a subsequent study, modification by addition of appendages, inspired by mastigoneme structures, perpendicular to the main helical flagellum of the microswimmer enabled additional control in swimming behavior.^[75] By increasing the ratio between length and interval of appendages, the swimming velocity can be decreased up to complete reversal of swimming direction.

One of the main issues of the presented approach is that due to the ferromagnetic property of the nickel surface, magnetization of the microstructures induces attractive forces between microswimmers causing formation of agglomerations, which are potentially prejudicial to prospective biomedical applications. To circumvent this problem, Tottori et al. demonstrated controlled assembly and disassembly of helical microswimmers in the presence of weak rotating magnetic fields by tuning direction, speed, and strength of it.^[76]

In the context of biomedical applications, biocompatibility and biodegradability of materials used for helical microswimmers must be ensured. In order to avoid nickel cytotoxicity, Qiu et al. reported helical microswimmers based on biocompatible ORMOCOMP photoresist and iron coating.^[65] To reduce corrosion of iron in aqueous biological environments,

an anticorrosive thin film of titanium was added. Cell compatibility tests revealed little cytotoxicity for C2C12 mouse myoblasts and enhancement in cell viability. A maximum forward speed of $49 \mu\text{m s}^{-1}$ was achieved at a magnetic induction of 9 mT and a frequency of 72 Hz.

In addition, photoresists containing superparamagnetic nanoparticles, avoiding in this way cytotoxic nickel coating, were also explored. Suter et al.^[67] prepared helical microswimmers using a magnetic polymer composite (MPC) photoresist composed of photocurable SU-8 resin and biocompatible magnetite nanoparticles. MPC structures containing up to 10 vol% nanoparticles showed no significant influence on cell viability.

In the previous example, the helical microrobots exhibited geometry-dependent magnetic properties due to statistically distributed nanoparticles within the printed structure. This shape anisotropy limits the device design as well as its efficient actuation. Peters et al. fabricated three different microrobot designs with shape independent properties by combination of two-photon polymerization and programmed anisotropy.^[68] There, an external field was applied during composite photoresist soft baking, aligning in this way superparamagnetic nanoparticles in chains representing the preferred direction for magnetization. The particles remained locked during lithography and subsequent processing, transferring particle alignment and directionality of particle anisotropy to the fabricated devices. Microrobots fabricated in this way were able to perform wobble-free rotation at low excitation frequencies and out-of-plane swimming.

In another example, Wang et al. designed biocompatible microswimmers based on nontoxic hydrogel gelatin methacryloyl.^[66] Incorporation of magnetic actuation was achieved by surface decoration with iron oxide nanoparticles. The swimmer was fully degradable by collagenases and was gradually digested by cell-released enzymes, producing noncytotoxic degradation products. Interestingly, the swimmers' forward velocity remained high after exceeding the step-out frequency. The authors attributed this abnormal locomotion behavior to the reduction of drag forces upon swimmer deformation at high magnetic frequencies.

Helical Microswimmers for Drug Delivery: Liposome-based helical microstructures as drug delivery systems were developed by the Nelson group. Thereby, liposomes serve as drug delivery vehicles able to encapsulate a drug and transport it into cells or release the drug in response to an external stimulus like temperature. Importantly, controlled drug delivery by helical microswimmers to single cells was demonstrated.^[70] The helical microstructures were surface functionalized with drug loaded liposomes, using Calcein as model drug and in vitro single cell drug delivery was tested on single C2C12 cells by cell imaging. A prerequisite for successful delivery to single cells was the contact between cell and functionalized microstructures. Calcein was exclusively delivered to the cell, which was in contact with the helical microswimmer. In another system reported by the same group, thermally controlled drug release was achieved by utilizing helical microswimmers functionalized with temperature sensitive liposomes, which exhibited a transition temperature at $41 \text{ }^\circ\text{C}$.^[77] The system was capable to incorporate hydrophilic and hydrophobic model drugs by liposome loading prior to printing. In particular, a thermally triggered Calcein release efficiency of $73 \pm 15\%$ was reported. Using similar conditions, the same

group demonstrated the preparation of helical microstructures capable of targeted gene transfer to mammalian cells based on lipoplex.^[78] Gene transfer ability was incorporated by surface decoration of microswimmers with lipoplexes containing encoding pDNA. Gene transfer to human embryonic kidney cells was confirmed by successful transfection to a parent cell and expression in two daughter cells. Thereby, transfection was locally limited to cells, which were in contact with the microswimmers.

In order to enable efficient medical treatment, delivery of an appropriate amount of drugs to the corresponding tissue sites is a mandatory. One possible solution is the deployment of precisely controlled helical microswimmer swarms, a requirement for in vivo control. Nelson and co-workers demonstrated for the first-time whole-body in vivo imaging of a swarm of helical microswimmers.^[79] The helical microswimmers were functionalized with near infrared probes, allowing deep tissue imaging. Using a set-up composed of three pairs of Helmholtz coils for generation of constant RMF combined with an IVIS optical imaging system swarms of up to 110 000 helical microswimmers were precisely controlled and monitored in vitro. In vivo swarm control and monitoring was performed with 80 000 microswimmers inside the peritoneal cavity of a mouse. In vivo velocity was significantly decreased due to the presence of proteins and bio-macromolecules. In a recent study, it was demonstrated that selective control of individual swimmers in a swarm was possible by tuning their surface chemistry.^[80] Printed helical microstructures were surface coated with nickel and gold and subsequently functionalized by thiol chemistry to render them either hydrophobic or hydrophilic. Raising its hydrophobicity led to an increase in the step-out frequency. This way selective control of helical microswimmers within a swarm was possible by variation of RMF input frequency.

By using the composite fabrication approach, i.e., by incorporating magnetic nanoparticles in the photoresist formulation, several microswimmer systems for targeted drug delivery were also developed. For example, Peters et al.^[81] reported a hydrolytically degradable microswimmer based on poly(ethylene glycol) diacrylate, pentaerythritol triacrylate (PETA) and iron oxide nanoparticles (**Figure 7**). Using a microfluidic test substrate, microswimmers successfully transported methylene blue, a model drug, to fixed cells. Upon release via passive diffusion, cells were successfully stained. Ester groups incorporated in the structure enabled efficient degradation by hydrolysis. Degradation products exhibited only low toxicity and possessed all excretion pathways. In a further study, Bozuyuk et al. fabricated a chitosan-based microswimmer system capable of light triggered drug release.^[82] The microswimmers were printed in a double-helix design. Doxorubicin, a model therapeutic, was linked via *o*-nitrobenzyl photolabile derivatives to the swimmer surface, enabling controlled drug release by using UV light. It was demonstrated that by irradiation with UV light in 1 min doses, 15% release of the incorporated drug amount per irradiation dose was achieved. In addition, partial degradation was possible in the presence of lysozyme after 204 h.

Ceylan et al. recently presented a hydrogel-based microswimmer capable of controlled cargo delivery in response to matrix metalloproteinase MMP-2.^[69] The microrobot was designed as cylindrical core wrapped up by a double helix with cones on both ends. The hydrogel material was fully degradable

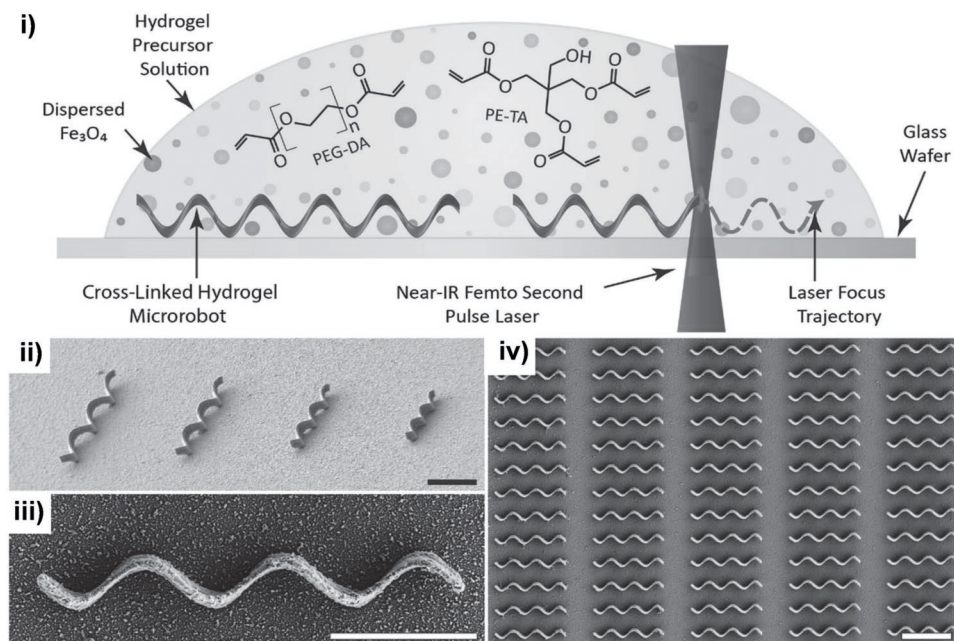


Figure 7. i) Schematic representation for the fabrication of magnetic microswimmers using 50/50 vol% PEGDA/PETA photoresist for 3D laser lithography; ii) SEM image of helical test patterns with diameters between 1.5 and 3.0 μm and lengths between 14 and 28 μm in a tilted SEM image; iii) SEM top-view of a helical microswimmer; iv) SEM top-view of an array of helical microswimmers. All scale bars are 10 μm . Adapted with permission.^[81] Copyright 2016, Wiley-VCH.

in the presence of MMP-2, typically overexpressed by cancer cells. The degradation process was accompanied by swelling of the drug-loaded microswimmer leading to drug release. Furthermore, complete microswimmer degradation gave access to release of the complete drug cargo. The remaining nanoparticles, functionalized with fluorophores and antibodies prior to printing, were used as cancer cell labeling agents after microswimmer degradation.

Micro-Object Manipulation: Another area of application for microrobots is micro-object manipulation, for controlled micro-assembly of objects or target delivery tasks. Strategies based on different microroboter designs, including helical^[64] and ciliary microrobots,^[83] were developed. Tottori et al. produced a helical microswimmer design featuring a microholder able to transport a microparticle across surfaces of different heights.^[64] One limitation was that only objects small enough to fit into the holder can be stably transported. Another general limitation of helical coated microswimmers is the presence of wobbling motion at low magnetic field rotation frequencies. The motion stabilizes to corkscrew motion at higher frequencies. However, due to associated higher velocities precise control and transport becomes challenging. In their work Huang et al. presented a new helical microswimmer design able to perform precise micro-object manipulation.^[84] The authors added on both ends of the helical body ring shaped structures, minimizing wobbling by increase of drag forces. By coating nickel of different thickness, they prepared two swimmer types with different step-out frequencies, enabling selective motion control by input frequencies. The robots were able to perform four different contact and noncontact object manipulation strategies as well as cooperative transport of a microbar.

4.2.2. Other Magnetic Microswimmers

In the previous examples employing metal coated helical microswimmers, the cargo is typically attached to the surface. Thus, drugs and cells are completely exposed to the fluidic environment leading to possible reactions between drugs and solvent or incompatibilities between attached cells and biological units. In order to protect the cargo from these environmental conditions, other geometries such as capsule-based microstructures were investigated.

Lee et al. reported a microtransporter consisting of two separate parts: a magnetically actuated helical plunger structure and a nonresponsive cylindrical cap.^[85] Such system allowed targeted drug and cell transport based on pick and drop motion. The plunger was composed of a helical tail for locomotion and a cylindrical open container to encapsulate cells or drug loaded particles. For loading, the plunger generates a vortex to encapsulate the particles in its cylinder and subsequently assembles with the cap, preventing loss of particles. After transport to the target area particles are released by opening the cap via an opposite RMF. The transporter can also be used to control the position of the cap after adhering of cells or drugs on the surface of it.

A promising microtransporter system that actively collects, encapsulates, transports and performs controlled release of microparticles and cells was reported by Huang et al.^[71] The transporter consists of a magnetically actuated freely rotatable main shaft inside a passive cylinder (**Figure 8**) The magnetic external screw allows corkscrew locomotion, whereas the internal Archimedean screw pump allows controlled uptake and release of particles. For particle uptake, the micropump

generates a recirculating flow, drawing particles through a filter on the front side into the chamber. During uptake and transport, a piston closes the rear site of the capsule to prevent particle loss. Upon release initiated by reversing the direction of the RMF, the piston opens and particles are expelled through a reverse flow generated by the pump. Applying the compartmentalization concept, the transporter was used for uptake, transport and release of smaller microswimmers in an artificial capillary network. The microswimmers were further navigated to smaller branches showing the systems potential for biomedical applications.

In the case of cell transport and cell loading, the capability of helical microswimmers is limited by their low surface area. For

a more efficient transport, 3D scaffold type microrobots were designed, displaying larger surface area. In one example, Kim et al. demonstrated printed hexahedral and cylindrical scaffold type microrobots for in vitro cell transport.^[86] For enhancement of cell attachment, a poly-L-lysine coating was added on the Ni/Ti bilayer. Human embryonic kidney cells were successfully cultivated inside the robots in vitro without cytotoxic effects after 96 h.

In another example, Li et al. demonstrated in vivo cell transport by noncytotoxic burr-like porous spherical microrobots.^[72] Microrobots were prepared with diameters ranging from 70 to 90 μm . In vivo cell transport was successfully performed and monitored in yolks of zebrafish embryos. During the

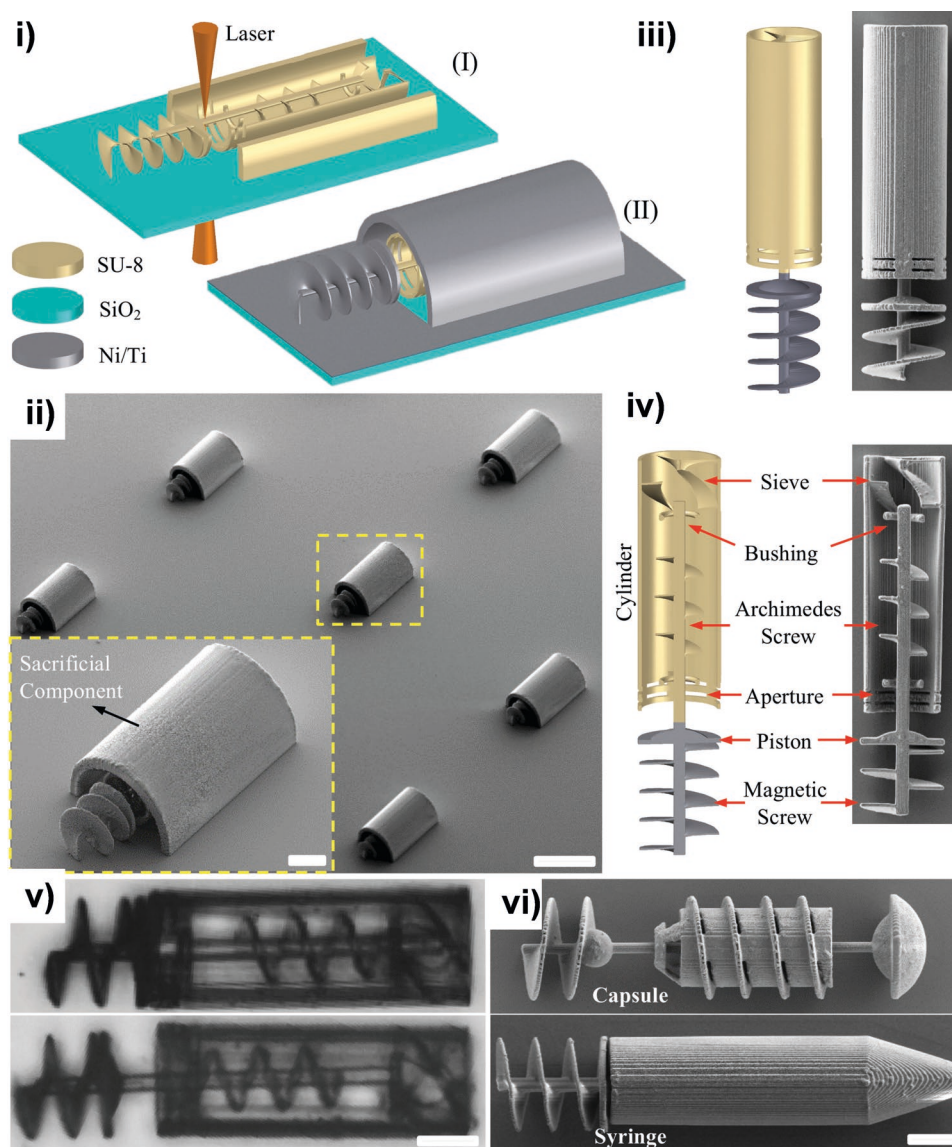


Figure 8. i) Schematic representation of the fabrication process of a microtransporter: I) 3D laser lithography of microstructures and II) selective physical vapor deposition of magnetic material; ii) Horizontal array of micromachines before the removal of sacrificial structures. The scale bars are 20 and 100 μm ; iii) Final product after the removal of the sacrificial structures. iv) The cross-sectional view of the microtransporter illustrating different mechanical components; v) Two different modes of the reciprocating mechanism (closed and open). The main shaft translates due to the rotation of the magnetic screw. vi) 3D printed microcapsule (top) and microsyringe (bottom) functioning with the same reciprocating mechanism. The scale bars in (v–vi) are 20 μm . Adapted with permission.^[71] Copyright 2015, Wiley-VCH.

experiment, the heartbeat of the zebrafish was observed indicating that it was alive. Injected loaded transporters (HeLa GFP+ cells) in the left dorsum of a mice resulted in a tumor after 4 weeks cultivation, confirming spontaneous cell release.

4.2.3. Synergic Systems: Magnetic Microstructures and Biological Cells

Another interesting concept is the combination of biological cells with 3D printed moieties, producing responsive multifunctional devices. Examples in which biological cells were used as functional units for drug delivery, fertilization and propulsion will be presented in the following part.

Medina-Sánchez et al. presented a sperm-carrying micromotor concept for in vivo artificial fertilization.^[87] The authors combined magnetically actuated helical Ni/Ti-coated microswimmers with immotile but otherwise functional sperm cells. Sperms were captured by these machines and transported to an oocyte. Unfortunately, sperm delivery was not always possible due to unspecific adhesion to the microhelix during release.

Applying sperm cells as propulsion source, Xu et al. demonstrated a sperm-hybrid micromotor concept for targeted drug delivery, aiming at a potential treatment for diseases in the female reproductive tract.^[88] Drug loaded sperm cells were combined with printed Fe/Ti coated tetrapod devices, which navigated the sperms to target cells. Design of the devices allowed liberation of sperm cells upon collision with a barrier. By subsequent cell fusion, drugs could be delivered directly to cells minimizing drug dilution into the extracellular matrix or body fluids. Application of the motors in vitro allowed successful treatment of HeLa tumor cells.

Using light as control stimulus, Vizsnyiczai et al. fabricated micromotors powered by bacteria.^[89] A micromotor consisting of a central rotating unit including microchambers for accommodation of bacteria, a central rotation axis and a radial ramp to facilitate capture of bacteria was printed from SU-8 resist. Capture of genetically designed light responsive *E. coli* bacteria enabled controlled rotation of the rotating unit in response to light intensity under inert conditions.

4.3. Outlook

Since the first printed example of a magnetically actuated microrobot in 2012, 3D laser lithography has been established as a suitable method for manufacturing of magnetic microrobots due to its high flexibility in terms of geometric versatility and material selection. A large variety of microswimmers, which offer a wide range of features such as selective swimmer control, as well as elaborated transport systems for drugs and cells were successfully created.

Although significant progress has been made in the field, almost all the systems based on composite structures are limited to magnetic materials. We believe that future combinations of new types of new responsive photoresists, especially photoreponsive materials, will allow for the creation of more sophisticated microrobots for complicated in vivo tasks.

5. Summary and Future Perspectives

During the last years, promising examples of defined 4D microstructures employing hydrogels, liquid crystals and composite materials have been shown. Stimuli-responsive monomers based on acrylamides, acrylates and few examples containing proteins have been successfully used for the preparation of soft structures exhibiting actuation mainly driven by a temperature or pH change in aqueous media (Section 2). Liquid crystalline-based materials have also been explored as good candidates to allow for actuation in the microscale and the first examples of simple microactuated robots have recently been shown (Section 3), in addition, elaborated magnetic microswimmers able to transport drugs and cells have been successfully demonstrated (Section 4).

Although a variety of stimuli-responsive microstructures has been reported, further efforts to include this concept in real life applications are needed. Thus, future work on efficiently controlling the response and adaptivity of the printed microstructures to external stimuli is essential. For example, the development of novel materials able to respond independently to more than one stimulus or microstructures where a truly spatially controlled response is achieved will allow for more degrees of freedom in the design and actuation of the microstructures.

Despite the outlined challenges, the emerging field of 4D microprinting has good prospects and we are optimistic that dynamic microstructures whose properties, e.g. shape, can be controlled on demand will have a big impact in the near future.

Acknowledgements

C.A.S., M.H., and A.M. contributed equally to this work. E.B. acknowledges funding from the Deutsche Forschungsgemeinschaft (DFG, German Research Foundation) via the project BL 1604/2-1. The authors acknowledge financial support from the Helmholtz program "Science and Technology of Nanosystems" (STN), from the DFG under Germany's Excellence Strategy via the Excellence Cluster 3D Matter Made to Order (EXC-2082 - 390761711), and by the Carl Zeiss Foundation through the "Carl-Zeiss-Focus@HEiKA." C.B.-K. acknowledges funding from the Australian Research Council (ARC) in the form of a Laureate Fellowship underpinning his photochemical research program as well as key continued support from the Queensland University of Technology (QUT). M.H. and A.M. acknowledge support by the Karlsruhe School of Optics and Photonics (KSOP).

Conflict of Interest

The authors declare no conflict of interest.

Keywords

4D printing, direct laser writing, hydrogels, liquid crystals, microrobots

Received: September 14, 2019

Revised: November 2, 2019

Published online:

[1] A. J. Capel, S. Edmondson, S. D. R. Christie, R. D. Goodridge, R. J. Bibb, M. Thurstans, *Lab Chip* **2013**, *13*, 4583.

[2] D. D. Gu, W. Meiners, K. Wissenbach, R. Poprawe, *Int. Mater. Rev.* **2012**, *57*, 133.

- [3] F. P. W. Melchels, M. A. N. Domingos, T. J. Klein, J. Malda, P. J. Bartolo, D. W. Hutmacher, *Prog. Polym. Sci.* **2012**, *37*, 1079.
- [4] S. D. Gittard, R. J. Narayan, *Expert Rev. Med. Devices* **2010**, *7*, 343.
- [5] a) S. C. Ligon, R. Liska, J. Stampfl, M. Gurr, R. Mülhaupt, *Chem. Rev.* **2017**, *117*, 10212; b) A. Bagheri, J. Jin, *ACS Appl. Polym. Mater.* **2019**, *1*, 593; c) A. Camposeo, L. Persano, M. Farsari, D. Pisignano, *Adv. Opt. Mater.* **2019**, *7*, 1800419.
- [6] S. Maruo, O. Nakamura, S. Kawata, *Opt. Lett.* **1997**, *22*, 132.
- [7] C. Barner-Kowollik, M. Bastmeyer, E. Blasco, G. Delaittre, P. Müller, B. Richter, M. Wegener, *Angew. Chem., Int. Ed.* **2017**, *56*, 15828.
- [8] M. Carlotti, V. Mattoli, *Small* **2019**, *15*, 1902687.
- [9] F. Momeni, S. M. M. Hassani, N. X. Liu, J. Ni, *Mater. Des.* **2017**, *122*, 42.
- [10] S. Naficy, R. Gately, R. Gorkin III, H. Xin, G. M. Spinks, *Macromol. Mater. Eng.* **2017**, *302*, 1600212.
- [11] C. M. González-Henríquez, M. A. Sarabia-Vallejos, J. Rodríguez-Hernández, *Prog. Polym. Sci.* **2019**, *94*, 57.
- [12] J. del Barrio, C. Sánchez-Somolinos, *Adv. Opt. Mater.* **2019**, *7*, 1900598.
- [13] M. A. C. Stuart, W. T. S. Huck, J. Genzer, M. Müller, C. Ober, M. Stamm, G. B. Sukhorukov, I. Szleifer, V. V. Tsukruk, M. Urban, F. Winnik, S. Zauscher, I. Luzinov, S. Minko, *Nat. Mater.* **2010**, *9*, 101.
- [14] M. Wei, Y. Gao, X. Li, M. J. Serpe, *Polym. Chem.* **2017**, *8*, 127.
- [15] M. Zarek, M. Layani, I. Cooperstein, E. Sachyani, D. Cohn, S. Magdassi, *Adv. Mater.* **2016**, *28*, 4449.
- [16] B. Jin, H. Song, R. Jiang, J. Song, Q. Zhao, T. Xie, *Sci. Adv.* **2018**, *4*, eaao3865.
- [17] D. Seliktar, *Science* **2012**, *336*, 1124.
- [18] E. Caló, V. V. Khutoryanskiy, *Eur. Polym. J.* **2015**, *65*, 252.
- [19] M. C. Koetting, J. T. Peters, S. D. Steichen, N. A. Peppas, *Mater. Sci. Eng., R* **2015**, *93*, 1.
- [20] A. M. Rosales, K. S. Anseth, *Nat. Rev. Mater.* **2016**, *1*, 15012.
- [21] C. de las Heras Alarcón, S. Pennadam, C. Alexander, *Chem. Soc. Rev.* **2005**, *34*, 276.
- [22] X.-J. Ju, L.-Y. Chu, X.-L. Zhu, L. Hu, H. Song, W.-M. Chen, *Smart Mater. Struct.* **2006**, *15*, 1767.
- [23] J. A. Shadish, G. M. Benuska, C. A. DeForest, *Nat. Mater.* **2019**, *18*, 1005.
- [24] L. Ionov, *Adv. Funct. Mater.* **2013**, *23*, 4555.
- [25] Z. Xiong, M.-L. Zheng, X.-Z. Dong, W.-Q. Chen, F. Jin, Z.-S. Zhao, X.-M. Duan, *Soft Matter* **2011**, *7*, 10353.
- [26] M. R. Lee, I. Y. Phang, Y. Cui, Y. H. Lee, X. Y. Ling, *Small* **2015**, *11*, 740.
- [27] L. D. Zarzar, P. Kim, M. Kolle, C. J. Brinker, J. Aizenberg, B. Kaehr, *Angew. Chem., Int. Ed.* **2011**, *50*, 9356.
- [28] L. D. Zarzar, J. Aizenberg, *Acc. Chem. Res.* **2014**, *47*, 530.
- [29] M. Hippler, E. Blasco, J. Qu, M. Tanaka, C. Barner-Kowollik, M. Wegener, M. Bastmeyer, *Nat. Commun.* **2019**, *10*, 232.
- [30] X. Huang, X. Wang, Y. Zhao, *Dyes Pigm.* **2017**, *141*, 413.
- [31] Z. Li, J. Torgersen, A. Ajami, S. Mühlleder, X. Qin, W. Husinsky, W. Holthöner, A. Ovsianikov, J. Stampfl, R. Liska, *RSC Adv.* **2013**, *3*, 15939.
- [32] D. Jin, Q. Chen, T.-Y. Huang, J. Huang, L. Zhang, H. Duan, *Mater. Today* **2019**, <https://doi.org/10.1016/j.mattod.2019.06.002>.
- [33] B. Kaehr, J. B. Shear, *Proc. Natl. Acad. Sci. USA* **2008**, *105*, 8850.
- [34] J. Qu, M. Kadic, A. Naber, M. Wegener, *Sci. Rep.* **2017**, *7*, 40643.
- [35] X. Kuang, J. Wu, K. Chen, Z. Zhao, Z. Ding, F. Hu, D. Fang, H. J. Qi, *Sci. Adv.* **2019**, *5*, eaav5790.
- [36] T. Watanabe, M. Akiyama, K. Totani, S. M. Kuebler, F. Stellacci, W. Wenseleers, K. Braun, S. R. Marder, J. W. Perry, *Adv. Funct. Mater.* **2002**, *12*, 611.
- [37] Z. Xiong, X.-Z. Dong, W.-Q. Chen, X.-M. Duan, *Appl. Phys. A* **2008**, *93*, 447.
- [38] A. Tudor, C. Delaney, H. Zhang, A. J. Thompson, V. F. Curto, G.-Z. Yang, M. J. Higgins, D. Diamond, L. Florea, *Mater. Today* **2018**, *21*, 807.
- [39] C. Lv, X.-C. Sun, H. Xia, Y.-H. Yu, G. Wang, X.-W. Cao, S.-X. Li, Y.-S. Wang, Q.-D. Chen, Y.-D. Yu, H.-B. Sun, *Sens. Actuators, B* **2018**, *259*, 736.
- [40] D. Serien, K. Sugioka, *Opto-Electron. Adv.* **2018**, *1*, 18000801.
- [41] P.-G. de Gennes, *The Physics of Liquid Crystals*, Oxford University Press, London, UK **1974**.
- [42] M. Warner, E. M. Terentjev, *Liquid Crystal Elastomers (International Series of Monographs on Physics)*, Vol. 120, Oxford University Press, Oxford, UK **2009**.
- [43] A. Kotikian, R. L. Truby, J. W. Boley, T. J. White, J. A. Lewis, *Adv. Mater.* **2018**, *30*, 1706164.
- [44] T. J. White, D. J. Broer, *Nat. Mater.* **2015**, *14*, 1087.
- [45] C. P. Ambulo, J. J. Burroughs, J. M. Boothby, H. Kim, M. R. Shankar, T. H. Ware, *ACS Appl. Mater. Interfaces* **2017**, *9*, 37332.
- [46] E. Sungur, M.-H. Li, G. Taupier, A. Boeglin, M. Romeo, S. Méry, P. Keller, K. D. Dorkenoo, *Opt. Express* **2007**, *15*, 6784.
- [47] H. Zeng, D. Martella, P. Wasylczyk, G. Cerretti, J.-C. G. Lavocat, C.-H. Ho, C. Parmeggiani, D. S. Wiersma, *Adv. Mater.* **2014**, *26*, 2319.
- [48] M. López-Valdeolivas, D. Liu, D. J. Broer, C. Sánchez-Somolinos, *Macromol. Rapid Commun.* **2018**, *39*, 1700710.
- [49] D. J. Roach, X. Kuang, C. Yuan, K. Chen, H. J. Qi, *Smart Mater. Struct.* **2018**, *27*, 125011.
- [50] F. C. Frank, *Discuss. Faraday Soc.* **1958**, *25*, 19.
- [51] A. M. Flatae, M. Burresti, H. Zeng, S. Nocentini, S. Wiegeler, C. Parmeggiani, H. Kalt, D. Wiersma, *Light: Sci. Appl.* **2015**, *4*, e282.
- [52] D. Martella, S. Nocentini, D. Nuzhdin, C. Parmeggiani, D. S. Wiersma, *Adv. Mater.* **2017**, *29*, 1704047.
- [53] S. Nocentini, F. Riboli, M. Burresti, D. Martella, C. Parmeggiani, D. S. Wiersma, *ACS Photonics* **2018**, *5*, 3222.
- [54] F. J. Kahn, *Appl. Phys. Lett.* **1973**, *22*, 386.
- [55] H. Zeng, P. Wasylczyk, C. Parmeggiani, D. Martella, M. Burresti, D. S. Wiersma, *Adv. Mater.* **2015**, *27*, 3883.
- [56] C. C. Tartan, P. S. Salter, T. D. Wilkinson, M. J. Booth, S. M. Morris, S. J. Elston, *RSC Adv.* **2017**, *7*, 507.
- [57] D. Martella, D. Antonioli, S. Nocentini, D. S. Wiersma, G. Galli, M. Laus, C. Parmeggiani, *RSC Adv.* **2017**, *7*, 19940.
- [58] R. A. M. Hikmet, D. J. Broer, *Polymer* **1991**, *32*, 1627.
- [59] H. Zeng, P. Wasylczyk, G. Cerretti, D. Martella, C. Parmeggiani, D. S. Wiersma, *Appl. Phys. Lett.* **2015**, *106*, 111902.
- [60] S. Nocentini, D. Martella, C. Parmeggiani, S. Zanutto, D. S. Wiersma, *Adv. Opt. Mater.* **2018**, *6*, 1800167.
- [61] E. Sungur, L. Mager, A. Boeglin, M.-H. Li, P. Keller, K. D. Dorkenoo, *Appl. Phys. A* **2010**, *98*, 119.
- [62] S. Zanutto, F. Sgrignuoli, S. Nocentini, D. Martella, C. Parmeggiani, D. S. Wiersma, *Appl. Phys. Lett.* **2019**, *114*, 201103.
- [63] T. Frenzel, M. Kadic, M. Wegener, *Science* **2017**, *358*, 1072.
- [64] S. Tottori, L. Zhang, F. Qiu, K. K. Krawczyk, A. Franco-Obregón, B. J. Nelson, *Adv. Mater.* **2012**, *24*, 811.
- [65] F. Qiu, L. Zhang, K. E. Peyer, M. Casarosa, A. Franco-Obregón, H. Choi, B. J. Nelson, *J. Mater. Chem. B* **2014**, *2*, 357.
- [66] X. Wang, X.-H. Qin, C. Hu, A. Terzopoulou, X.-Z. Chen, T.-Y. Huang, K. Maniura-Weber, S. Pané, B. J. Nelson, *Adv. Funct. Mater.* **2018**, *28*, 1804107.
- [67] M. Suter, L. Zhang, E. C. Siringil, C. Peters, T. Luehmann, O. Ergeneman, K. E. Peyer, B. J. Nelson, C. Hierold, *Biomed. Micro-devices* **2013**, *15*, 997.
- [68] C. Peters, O. Ergeneman, P. D. W. García, M. Müller, S. Pané, B. J. Nelson, C. Hierold, *Adv. Funct. Mater.* **2014**, *24*, 5269.
- [69] H. Ceylan, I. C. Yasa, O. Yasa, A. F. Tabak, J. Giltinan, M. Sitti, *ACS Nano* **2019**, *13*, 3353.
- [70] R. Mhanna, F. Qiu, L. Zhang, Y. Ding, K. Sugihara, M. Zenobi-Wong, B. J. Nelson, *Small* **2014**, *10*, 1953.
- [71] T.-Y. Huang, M. S. Sakar, A. Mao, A. J. Petruska, F. Qiu, X.-B. Chen, S. Kennedy, D. Mooney, B. J. Nelson, *Adv. Mater.* **2015**, *27*, 6644.

- [72] J. Li, X. Li, T. Luo, R. Wang, C. Liu, S. Chen, D. Li, J. Yue, S.-h. Cheng, D. Sun, *Sci. Rob.* **2018**, *3*, eaat8829.
- [73] E. M. Purcell, *Am. J. Phys.* **1977**, *45*, 3.
- [74] A. W. Mahoney, N. D. Nelson, K. E. Peyer, B. J. Nelson, J. J. Abbott, *Appl. Phys. Lett.* **2014**, *104*, 144101.
- [75] S. Tottori, B. J. Nelson, *Biomicrofluidics* **2013**, *7*, 061101.
- [76] S. Tottori, L. Zhang, K. E. Peyer, B. J. Nelson, *Nano Lett.* **2013**, *13*, 4263.
- [77] F. Qiu, R. Mhanna, L. Zhang, Y. Ding, S. Fujita, B. J. Nelson, *Sens. Actuators, B* **2014**, *196*, 676.
- [78] F. Qiu, S. Fujita, R. Mhanna, L. Zhang, B. R. Simona, B. J. Nelson, *Adv. Funct. Mater.* **2015**, *25*, 1666.
- [79] A. Servant, F. Qiu, M. Mazza, K. Kostarelos, B. J. Nelson, *Adv. Mater.* **2015**, *27*, 2981.
- [80] X. Wang, C. Hu, L. Schurz, C. De Marco, X. Chen, S. Pané, B. J. Nelson, *ACS Nano* **2018**, *12*, 6210.
- [81] C. Peters, M. Hoop, S. Pané, B. J. Nelson, C. Hierold, *Adv. Mater.* **2016**, *28*, 533.
- [82] U. Bozuyuk, O. Yasa, I. C. Yasa, H. Ceylan, S. Kizilel, M. Sitti, *ACS Nano* **2018**, *12*, 9617.
- [83] S. Kim, S. Lee, J. Lee, B. J. Nelson, L. Zhang, H. Choi, *Sci. Rep.* **2016**, *6*, 30713.
- [84] T.-Y. Huang, F. Qiu, H.-W. Tung, K. E. Peyer, N. Shamsudhin, J. Pokki, L. Zhang, X.-B. Chen, B. J. Nelson, M. S. Sakar, *RSC Adv.* **2014**, *4*, 26771.
- [85] S. Lee, S. Kim, S. Kim, J.-Y. Kim, C. Moon, B. J. Nelson, H. Choi, *Adv. Healthcare Mater.* **2018**, *7*, 1700985.
- [86] S. Kim, F. Qiu, S. Kim, A. Ghanbari, C. Moon, L. Zhang, B. J. Nelson, H. Choi, *Adv. Mater.* **2013**, *25*, 5863.
- [87] M. Medina-Sánchez, L. Schwarz, A. K. Meyer, F. Hebenstreit, O. G. Schmidt, *Nano Lett.* **2016**, *16*, 555.
- [88] H. Xu, M. Medina-Sánchez, V. Magdanz, L. Schwarz, F. Hebenstreit, O. G. Schmidt, *ACS Nano* **2018**, *12*, 327.
- [89] G. Vizsnyiczai, G. Frangipane, C. Maggi, F. Saglimbeni, S. Bianchi, R. Di Leonardo, *Nat. Commun.* **2017**, *8*, 15974.